Synthesis of Chitosan Coated Iron Oxide (Fe_3O_4) Nanoparticles by Electrochemical Method

A THESIS SUBMITTED IN PARTIAL FULFILMENT OF THE REQUIREMENT FOR THE DEGREE OF

Bachelor in Technology

in

Biotechnology

by

Lipsa Kumari Goel (111BT0531)
&
Abhipsa Mishra (111BT0577)

Department of Biotechnology and Medical Engineering,
National Institute of Technology,
Rourkela.

Synthesis of Chitosan Coated Iron Oxide (Fe_3O_4) Nanoparticles by Electrochemical Method

A THESIS SUBMITTED IN PARTIAL FULFILMENT OF THE REQUIREMENT FOR THE DEGREE OF

Bachelor in Technology

in

Biotechnology

by

Lipsa Kumari Goel (111BT0531)
&
Abhipsa Mishra (111BT0577)

Under the Guidance of

Dr. Amit Biswas

Department of Biotechnology and Medical Engineering,
National Institute of Technology,
Rourkela.

CERTIFICATE

This is to certify that the thesis entitled '**Synthesis of Chitosan Coated Iron Oxide (Fe3O4) Nanoparticles by Electrochemical Method'** submitted by **Lipsa Kumari Goel** and **Abhipsa Mishra** in partial fulfilment of the requirements for the award of Bachelor of Technology from the Department of Biotechnology and Medical Engineering with specialization in "Biotechnology Engineering" at National Institute of Technology, Rourkela (Deemed University) is an authentic work carried out by them under my supervision and guidance. To the best of my knowledge, the matter embodied in the thesis has not been submitted to any other University/Institute for the award of any degree or diploma.

Place:

Date:

Supervisor
Dr. Amit Biswas
Department of Biotechnology and Medical Engineering,
National Institute of Technology, Rourkela- 769008.

ACKNOWLEDGEMENT

We would like take this opportunity to express our deep gratitude and thank all those who have been instrumental in the successful completion of our project.

We thank Dr. Amit Biswas, Assistant Professor in the Department of Biotechnology and Medical Engineering, NIT Rourkela, for providing us with the opportunity to work on this project. His steady guidance and patient mentoring has proven to be invaluable during our work period. We would also like to express our heartfelt gratitude to Mr. Bhishamnarayan Singh, Mr. K. Senthilguru, Mr. Gautham Harinarayana, Ms. Yamini Yogalakshmi and Mr. Niladri Panda for their priceless insights without which this project would not have seen a successful completion.

An honourable mention goes to our beloved friends for their continued care and help which went a long way in instilling in us a sense of enthusiasm that proved indispensable during the work period.

We thank all the knowledgeable faculty of the department and our lab mates at the Biomaterials and Tissue Engineering Laboratory for assisting us in our project.

Lipsa Kumari Goel Abhipsa Mishra

Date:

Place:

ABSTRACT

The increased interest in hybrid nanomaterials is due to the combined uses of the unique properties of both organic and inorganic component in a single material. In this class, magnetic polymer nanomaterials are of major interest because of the combination of excellent magnetic properties, stability, and good biocompatibility. Iron oxide nanoparticles can be utilized for multiple biotechnological and biomedical applications, but the major drawbacks of using these nanoparticles is their low stability and uneven size distribution due to the formation of agglomerates in aqueous solution. Thus, for application in various processes, iron oxide nanoparticles are coated with biocompatible polymers, mostly polysaccharides. The size plays an important role in the chemical and kinetic processes involved in the procedure. The final size of the coated particle is determined by the type of coating undertaken for modification of the surface properties according to the application it would be used for. The coated magnetic nanoparticles should enable localization of particles to a pre-defined area. It should be able to bind to the desired compound in such a manner that it can be controlled using an external magnetic field. In the current study, magnetic Fe_3O_4–chitosan nanoparticles were prepared by the covalent binding of chitosan (CTS) onto the surface of magnetic Fe_3O_4 nanoparticles which were prepared by electrochemical synthesis. The study aimed at the optimization of the electrochemical synthesis of iron oxide nanoparticles, their subsequent coating with chitosan and their utilization in environmental and biomedical applications.

Keywords: *Magnetic iron oxide nanoparticles, chitosan, coating, arsenic, anti-microbial activity*

LIST OF CONTENTS

Chapter 1: Introduction **1**

Chapter 2: Literature Review **5**

Objective **10**

Working Plan **11**

Chapter 3: Materials and Methods

3.1 Materials and Chemicals Required **13**

3.2 Methods **14**

Chapter 4: Results and Discussions

4.1 Dynamic Light Scattering **22**

4.2 Field Emission Scanning Electron Microscopy **27**

4.3 Zeta Potential **28**

4.4 Characterization and comparison of chitosan coated nanoparticles **30**

4.5 X-Ray Diffraction analysis **32**

4.6 Arsenic removal from water using chitosan coated iron oxide nanoparticles **34**

4.7 Anti-microbial activity of uncoated and coated nanoparticles **36**

4.8 Protein adsorption **37**

Chapter 5: Conclusion and Future Scope **41**

Chapter 6: References **42**

LIST OF FIGURES

Fig 1: Iron oxide particles obtained under different processing conditions by electrolysis 14

Fig 2: Washing of nanoparticles with ethanol 16

Fig 3: Size vs. Intensity data obtained from DLS for 0.1M LiCl, 3V, 15min 22

Fig 4: Size vs. Intensity data obtained from DLS for 0.2M LiCl, 1V, 15min 22

Fig 5: Size vs. Intensity data obtained from DLS for 0.2M LiCl, 2V, 15min 23

Fig 6: Size vs. Intensity data obtained from DLS for 0.2M LiCl, 3V, 15min 23

Fig 7: Size vs. Intensity data obtained from DLS for 0.3M LiCl, 1V, 15min 23

Fig 8: Size vs. Intensity data obtained from DLS for 0.3M LiCl, 2V, 15min 24

Fig 9: Size vs. Intensity data obtained from DLS for 0.3M LiCl, 3V, 15min 24

Fig 10: Size vs. Intensity data obtained from DLS for 0.3M LiCl, 2V, 30mins (ethanol washed samples) 25

Fig 11: Size vs. Intensity data obtained from DLS for 0.3M LiCl, 3V, 30mins 26

Fig 12: FESEM images of Fe_3O_4 nanoparticles synthesized by electrochmical method (0.3M, 2V) under different magnifications : a) 100k x and b) 200k x. 27

Fig 13: FESEM images of Fe_3O_4 nanoparticles synthesized by electrochmical method (0.3M, 3V) at 100k x magnification 28

Fig 14: Zeta Potential distribution for 0.3M 2V 29

Fig 15: Zeta Potential distribution for 0.3M 3V 29

Fig 16: Size vs. Intensity data obtained from DLS for chitosan coated nanoparticles with process parameters 2V, 0.3M 30

Fig 17: FESEM images of Fe_3O_4 nanoparticles with process parameters 0.3M, 2V in (a) uncoated and (b) coated conditions at 200k x magnification. 31

Fig 18: Zeta potential distribution for coated sample 31

Fig 19: XRD pattern of Fe_3O_4 nanoparticles for 2V, 0.2M 32

Fig 20: XRD pattern of Fe_3O_4 nanoparticles for 0.3M, 1V **33**

Fig 21: XRD pattern of Fe_3O_4 nanoparticles for 0.3M, 2V **33**

Fig 22: XRD pattern of Fe_3O_4 nanoparticles for 0.3M, 3V **34**

Fig 23: Standard curve for As_2O_3 **35**

Fig 24: Anti-microbial activity **36**

LIST OF TABLES

Table 1: Size distribution measurement of the nanoparticles by DLS **25**

Table 2: Size distribution measurement of the screened nanoparticles by DLS **26**

Table 3: Zeta Potential distribution analysis **29**

Table 4: Size distribution measurement of the chitosan coated nanoparticles by DLS **30**

Table 5: Zeta Potential distribution for coated samples **32**

Table 6: OD data obtained at 220.4nm **35**

Table 7: Reduction of As_2O_3 concentration after addition of coated iron oxide nanoparticles **36**

Table 8: Standard values for protein adsorption taken with BSA **37**

Table 9: OD values for uncoated nanoparticles **38**

Table 10: OD values for coated nanoparticles **39**

ABBREVIATIONS

°C	degree Celsius (Temperature)
µm	micro meter
As_2O_3	Arsenic Trioxide
BSA	Bovine Serum Albumin
DLS	Dynamic Light Scattering
Fe_3O_4	Iron Oxide
FESEM	Field Emission Scanning Electron Microscopy
HCl	Hydrochloric Acid
LiCl	Lithium Chloride
M	Molar
min	Minute
ml	mili liter
nm	nano meter
Nps	Nanoparticles
V	Volt
XRD	X-Ray Diffraction

CHAPTER 1:
INTRODUCTION

INTRODUCTION

When a particle which makes up a powder, cluster or crystal, has at least one dimension less than 100nm, the particle is called as a “nanoparticle”. The properties of the materials change when the particles composing it start approaching the nanoscale range. The properties of materials change as their size approaches the nanoscale because the percentage of atoms at the surface of the material becomes significant. This leads to a large surface area to volume ratio which subsequently decreases the temperature at which the nanoparticles just start to melt. The interaction of the particle surface with the solvent, which is strong enough for overcoming differences in density, enable the preparation of suspensions of nanoparticles. Sixteen pure phases of iron oxides, particularly, oxides such as Magne- tite, Hematite, Iron oxide beta phase and Maghemite, hydroxides such as Iron(III) hydroxide or Bernalite, Iron(II) hydroxide, oxy-hydroxides such as Geothite, Akaganetite, Lepidocrocite, Feroxy- hyte are known to date (1). Trivalent state, distinct colors and low solubility are characteristics of these compounds. One of the most important iron oxide, black in colour and ferromagnetic, is Magnetite (Fe_3O_4)

which contains both Fe(II) and Fe(III). An inverse spinel crystal structure is characteristic of magnetite (2). Various methods applied like gas phase methods, sol–gel technique, high-pressure hydro thermal or liquid phase methods, have been developed for the synthesis of magnetite or maghemite nanoparticles (3).

Small iron oxide particles have been applied in *in vitro* diagnostics for almost 40 years (4). In the last decade, increased investigations with several types of iron oxides have been carried out

in the field of nanosized magnetic particles (mostly maghemite, γ-Fe_2O_3, or magnetite, Fe_3O_4,

single domains of about 5–20 nm in diameter), among which magnetite is a very promising candidate since its biocompatibility has already been proven. Magnetic nanoparticles have effective and interesting applications in the fields of biomedicine, information technology,

magnetic resonance imaging, catalysis, telecommunication, and environmental remediation and have thus generated sufficient research interest (6-9). Magnetic nanocomposites generally comprise of magnetic nanoparticles embedded in nonmagnetic or magnetic matrix (10, 11).

However, magnetic nanoparticles usually have a strong tendency to form agglomerates for reduction of energy associated with high surface area-to-volume ratio of the nanosized particles. Coating the nanoparticles with a polymeric organic compound or with an inorganic layer is one way to avoid the aggregation of magnetic nanoparticles and enhance their chemical stability (12, 13).

Coating of nanoparticles also makes them possess the combined properties of high magnetic saturation, biocompatibility and interactive functions at the surface, thus leading to surface modification capable of further functionalization by the attachment of various bioactive molecules (15). Super-paramagnetic particles do not detain any magnetism after removal of external magnetic field and are thus of particular interest.

Surface modifications of iron oxide nanoparticles not only makes them chemically more stable but also makes them biocompatible for biomedical applications. For biomedical applications, iron oxide nanoparticles often treated with surface modification. Modification of the surface of iron oxide nanoparticles can be done by using a variety of materials like precious metals, silica, carbon and biopolymers (18–21). For the current study, chitosan has been chosen as the biopolymer of interest for coating purposes. Chitosan is a partially acetylated glucosamine biopolymer with characteristics like hydrophilicity, biocompatibility and biodegradability (22, 23). It also has amino groups which can be used for many functions along with specific functional groups or binding sites or chemical components which makes it an appropriate compound to be used for coating the iron oxide nanoparticles. Many investigations on chitosan modified magnetic nanoparticles used for biomedical applications have been reported.

In the present study, iron oxide–chitosan nanoparticles were obtained using iron oxide nanoparticles as cores and chitosan as the polymeric shell. Firstly, iron oxide nanoparticles were prepared by electrochemical process, then the iron oxide nanoparticles were adequately powdered homogenously and added to chitosan solution by appropriate proportion with reverse-phase suspension cross-linking method to form the magnetic nanoparticles with amine group. The coated nanoparticles were analysed for surface properties and characteristics using X-Ray Diffraction Crystallography, Dynamic Light Scattering, Fourier Transform Infrared Spectroscopy, Field Emission Scanning Electron Microscopy and Zeta Potential analysis. The coated nanoparticles were checked for applications in the removal of arsenic from waste water and for their anti-microbial activity.

CHAPTER 2:
LITERATURE REVIEW

LITERATURE REVIEW

2.1 Synthesis of Iron Oxide Nanoparticles

Magnetic iron oxide nanoparticles, mostly magnetite (Fe_3O_4) and maghemite (γ-Fe2O3), form an integral part of half metallic materials because they provide extensive possibilities and applications in biomedicine, research and separation processes. This can be attributed to their unique properties of superparamagnetism and biocompatibility. Iron oxide nanoparticles can be easily synthesized and the high surface area to volume ratio and smooth coating process and improved functionality increase their adaptability. (25,26) The main aim of any synthesis procedure for iron oxide nanoparticles is the optimization of the physical and chemical parameters of the process so as to control the size, shape, morphology and magnetic properties of the nanoparticles. This leads to a homogenously dispersed solution of the nanoparticles. But due to the presence of hydrophobic surfaces and the existence of a large surface-to-volume ratio, the nanoparticles during and after synthesis tend to form aggregate clusters, leading to the creation of uneven size distribution patterns. Various methods have been studied for the effective synthesis of iron oxide nanoparticles. Some notable studies are included below:

2.1.1 Co-precipitation method

In this process, iron oxide nanoparticles are precipitated from aqueous solutions of ferrous and ferric salts with alkali along with appropriate aging time. This method provides a large amount of nanoparticles but due to extensive agglomeration, particle size controlling becomes difficult (27).

2.1.2 Hydrothermal method

This is one of the most popular techniques for the synthesis of magnetic nanoparticles. The reactions are carried out in aqueous media at a temperature of 200°C and a high pressure of 200psi. The method is furthered by any of the following three techniques: hydrolysis, oxidation or neutralization of mixed metal hydroxides resulting in ferrite formation. The first two techniques are commonly followed as they are simpler to perform. The size of the particles produced during the hydrothermal method can be controlled by controlling the water content in the reaction mixture, reaction temperature and reaction time. (28, 29).

2.1.3 Microemulsion technique

This technique consists of three phases of oil, water and surfactant. Microemulsions are transparent, thermodynamically stable, liquid mixtures of oil, water and surfactant, frequently in combination with a co-surfactant. The surfactants aid in decreasing the surface tension between the continuous and immiscible phases thus keeping the various liquids present in the microemulsion stable. Varying the concentrations of the surfactants and the dispersed phase, the size of the droplets containing the iron oxide nanoparticles can be controlled and dispersed in the solution. The shapes and structures of the nanoparticles can even be controlled using this method. (30).

2.1.4 Sol-gel method

By this method, a “sol” of nanoparticles is prepared by the hydroxylation and subsequent condensation of precursor in solution. Further condensation and inorganic polymerization forms a three dimensional metallic oxide network which is called as “wet gel”. The properties of the gel is characteristic of the structure obtained within the sol stage. All processes were

carried out at ambient conditions but additional heat treatments are necessary for acquiring a fine crystalline state. (35, 36)

2.2 Chitosan coated iron oxide nanoparticles

Iron oxide nanoparticles tend to form agglomerates because of their high magnetic and hydrophobic activity with each other. Thus, to increase their functionality and make the most of their unique properties, it becomes imperative to coat them or make composites with various available biopolymers or inorganic compounds. Coating the naked iron oxide nanoparticles with chitosan, which is a hydrophilic, non-toxic, biodegradable and biocompatible polymer, enhances their stability in aqueous and colloidal solutions as well as in their dry state. Chitosan has a remarkable film forming characteristic and it's permeability towards water is also quite high. In addition, chitosan is a readily available cost effect biopolymer. The increased interest in the chitosan coated– Fe_3O_4 nanoparticles is because the resultant surface modification enhances their covalent attachment, self-assembly and organization on surfaces. (37, 38)

2.3 Arsenic removal from waste water

Arsenic is widely known as a toxic material and is most commonly found contaminating groundwater. Consumption of arsenic contaminated water on a regular basis can lead to various dangerous diseases like hyperpigmentation, skin cancer, liver cancer and circulatory disorders The World Health Organization (WHO) has directed a threshold value of 0.01 mg/L for arsenic in drinking water. The most popular methods for removing arsenic from water include adsorption-coprecipitation with hydrolyzing metals like aluminium or iron (III), adsorption on activated alumina or activated carbon, ion exchange, and reverse osmosis. But the most effective method for arsenic removal is by coagulation with iron salts and is used in large scale

treatment plants. (39) Iron oxide nanoparticles have been used to remove arsenate and arsenite from contaminated water using column studies (40).

2.4 Anti-microbial activity of iron oxide nanoparticles

Iron oxide-based nanomagnets have attracted a great deal of attention in nanomedicine over the past decade. Down to the nanoscale, superparamagnetic iron oxide nanoparticles can only be magnetized in the presence of an external magnetic field, which makes them capable of forming stable colloids in a physio-biological medium. Their superparamagnetic property, together with other intrinsic properties, such as low cytotoxicity, colloidal stability, and bioactive molecule conjugation capability, makes such nanomagnets ideal in both in-vitro andin-vivo biomedical applications. The growing interest in iron oxide-based nanomagnets with multifunctionalities was explored in cancer diagnostics and treatment, focusing on their combined roles in a magnetic resonance contrast agent, hyperthermia, and magnetic force assisted drug delivery. Iron oxides as magnetic carriers in gene therapy were reviewed with a focus on the sophisticated design and construction of magnetic vectors. Nanotopographies can be designed to promote or reduce cell adhesion and alter stem cell fate, all of which would be useful attributes for a range of applications in regenerative medicine, including orthopaedics and dentistry. Chemical surface patterning of implants could induce these effects, but topographies should persist better than chemical modification on the devices.

OBJECTIVE

The objective of the current study was the synthesis of iron oxide nanoparticles by electrochemical method, their coating with chitosan and the subsequent characterization of their physical properties. The entire process of the synthesis was optimized so that it becomes cost-effective. The objectives that were followed during this project are as follows:

1. Synthesis of iron oxide nanoparticles by electrochemical method
2. Characterization of the obtained iron oxide nanoparticles
3. Coating of the nanoparticles by a suitable method
4. Comparative study of the coated and uncoated nanoparticles by characterization techniques
5. Application of the chitosan coated nanoparticles for arsenic removal from water and anti-microbial activity

The characterization techniques undertaken during the project are:

1. Dynamic Light Scattering (DLS)
2. Zeta Potential Analysis
3. X-Ray Diffraction Crystallography (XRD)
4. FESEM (Field Emission Scanning Electron Microscopy)

WORKING PLAN

Synthesis of iron oxide nanoparticles using mild steel electrodes

↓

Optimization of electrolytic bath (LiCl) and voltage

↓

Selection on the basis of physical characteristics

↓

Particle size analysis using DLS

↓

Morphological study by FESEM

↓

Zeta Potential Analysis of uncoated nanoparticles

↓

Coating of iron oxide nanoparticles

↓

Particle size analysis for coated nanoparticles using DLS

↓

Morphological study of coated nanoparticles by using FESEM

↓

Zeta Potential Analysis of coated nanoparticles

↓

(a) Role of coated nanoparticles in removal of arsenic from water

(b) Antimicrobial activity of coated nanoparticles

CHAPTER 3:
MATERIALS AND METHODS

3.1 Materials and Chemicals Required

Various chemicals procured under laboratory grade for the current study are listed below:

3.1.1 Synthesis of iron oxide nanoparticles:

1. Electrodes: Mild Steel (0.5-0.6% Carbon) (5.2 x 2.3 x 0.4 cm^3)
2. Electrolyte: LiCl (98%, Avra)

3.1.2 Coating of nanoparticles:

1. Chitosan (Hi-Media)
2. Ethanol (Changshu Yangyuan Chemicals, China)

3.1.3 Other chemicals:

1. Arsenic Trioxide (Loba Chemie Pvt. Ltd.)
2. Glacial Acetic Acid (Hi-Media)
3. Luria Bertani Broth (Hi-Media)
4. Agar (Hi-Media)
5. Metrinidazole (Sigma-Aldrich)
6. Bovine Serum Albumin (Hi-Media)
7. Bradford reagent (Hi-Media)

3.2 Methods

3.2.1 Electrochemical synthesis of nanoparticles

A 2-electrode system was used for the electrochemical process. Two well-cut mild steel pieces having dimensions 5.2 x 2.3 x 0.4 cm^3 are taken. They were polished and grinded till there was no trace of any rust on them and the surfaces were shiny and smooth. These pieces acted as the anode and cathode respectively. They were connected to a DC power source. LiCl solution was prepared at a concentration of 0.1M and 100ml of it was taken in a glass beaker to act as the electrolyte for the process. The electrodes were carefully aligned inside the beaker so that they were partially dipped inside the electrolyte and were facing parallel to each other in an upright manner. The DC supply was provided by a device procured from APLAB and the DC power supply was such that its voltage could be modulated between 0-30V. The electrolytic process was carried out for 15min at 1V, 2V and 3V respectively. The process was repeated for 0.2M and 0.3M concentrations of LiCl. A total of 9 samples were obtained by the end of this process.

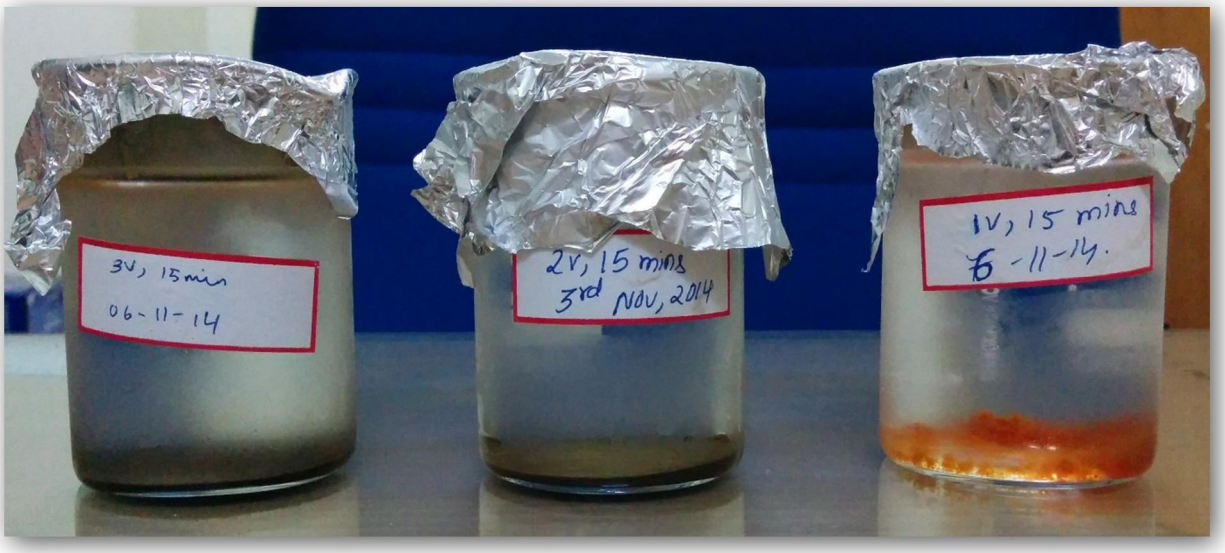

Fig 1: Iron oxide particles obtained under different processing conditions by electrolysis

The electrodes were cleaned and polished before every process that was carried out. The electrolytic process was carried out for a longer duration in case the amount of samples required was more.

The processes carried out for 0.1M LiCl at 1V and 2V were rejected because of the less amount of deposition observed after completion of the electrolytic process.

3.2.2 Dynamic Light Scattering

The samples obtained from the electrolytic process were left undisturbed overnight, allowing the nanoparticles to agglomerate and settle. About 1-2 ml of each of the 7 samples were taken and dispersed in distilled water and sonicated for about 9-12mins each. This ensured the breaking up of the agglomerates into nanoparticles. These 7 samples were analysed by Dynamic Light Scattering for a rough idea of the particle size distribution present in the samples. The results and graphs obtained are discussed in the forthcoming chapter.

It was observed that the best intensity of nanoparticles were obtained in the samples taken from the electrolytic processes having electrolytic concentration of 0.3M carried out at 2V and 3V. These samples were picked out for further analysis.

Ethanol washing: The sample to be washed was taken in a beaker and a magnetic bead wrapped with parafilm was dropped into it. About 100ml of 70% ethanol was added to 100ml of the sample. The beaker was covered with an aluminium foil and placed on a magnetic stirrer and was continuously stirred for 7-8 hours. After the washing was complete, the nanoparticles were allowed to settle down and form agglomerates. The clear liquid present on top of sediments was carefully removed with a pipette or dropper making sure that the bottom layer of nanoparticles is not disturbed at all. The iron oxide nanoparticles obtained from the electrolytic processes having electrolytic concentration of 0.3M carried out at 2V and 3V were

washed with 70%, 80%, 90% and 100% ethanol. Each washing was carried out for atleast 7-8 hours to ensure that the nanoparticles were free from all traces of LiCl.

After the wash with 100% ethanol was complete, the aluminium foil was removed from the beaker and the beaker was kept at 50-55°C for evaporation of the liquid present along with the nanoparticles. The evaporation was carried out for about 4-5hours, ensuring that the liquid did not start boiling at any point of time, regulating the temperature accordingly.

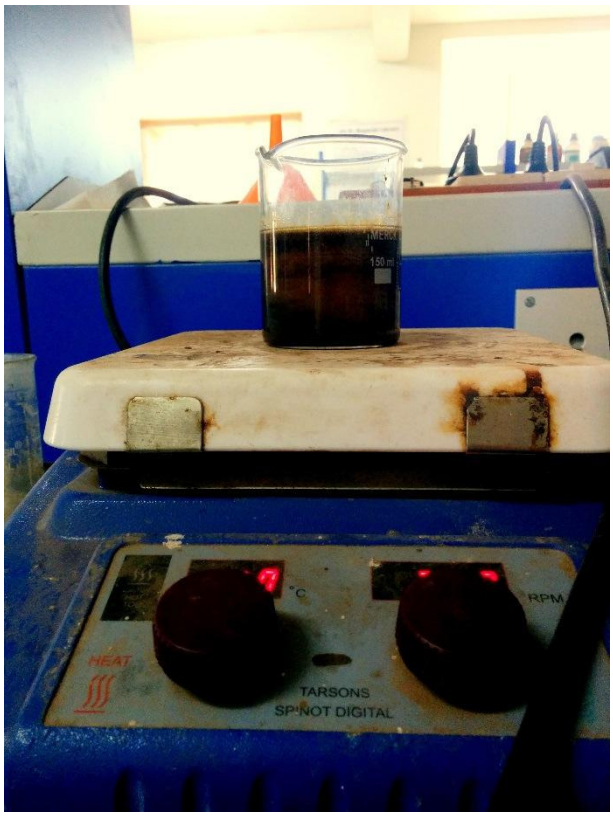

Fig 2: Washing of nanoparticles with ethanol

When the particles present inside the beaker looked completely dry, it was allowed to cool off before the particles were scrapped from the bottom and sides of the beaker. The scrapped particles were transferred to a mortar and ground till their texture resembled a free flowing powder. The powder was transferred to a screw cap vial and kept under air-tight conditions.

This powder was dispersed in about 10ml of distilled water and sonicated for 9mins and analysed with DLS again. Nanoparticles were found to be in the range of 200-250 nm.

For all DLS procedures, the count rate was 287.9 kcps and the duration of the processes was 60s.

Zeta Potential determination was done for the samples along with the particle size distribution using DLS.

3.2.3 X-Ray Diffraction

X-ray diffraction was conducted for the uncoated iron oxide nanoparticles with a Cu target as the X-Ray source (CuK-radiation). X-Ray intensity was measured for angles (2ϑ) in the range 30°-80° with scan rate of 2° per minute. The device used was X'PERT PANalytical X-Ray Diffractometer. The data obtained was plotted with Origin software and analysed for the characteristic readings of Fe_3O_4.

3.2.4 FESEM Analysis

The samples were prepared by electrochemical method and then kept undisturbed for 30mins. Using a pipette, a few drops of the supernatant was taken out. The nanoparticles remain dispersed in the liquid, thus the drops taken from the supernatant contain the particles needed for analysis. The drops were put on 4-5 glass slides. The glass slides were kept in a vacuum dryer and the liquid was allowed to evaporate. The particles were dried and deposited on the slides, which were taken for FESEM analysis.

3.2.5 Chitosan Coating of Iron Oxide Nanoparticles

The iron oxide nanoparticles were washed with ethanol and completely dried. It was ensured that they were in a powdered form. 1M acetic acid was prepared by adding 5.7ml of glacial

acetic acid, obtained from Hi-Media, to 100ml of distilled water. 20 mg of Chitosan, obtained from Hi-Media, was dissolved in the 100ml of 1M acetic acid. For coating purposes, 70mg of the iron oxide nanoparticles was dispersed in the chitosan solution in a vessel with a wide base to ensure effective coating. The vessel was kept on a shaker for nearly 18hours. A dark drown suspension is obtained after 18 hours. Then, the liquid was evaporated from the vessel by heating it at 50-55°C. The particles deposited on the surfaces and bottom of the flask were scrapped off using a clean spatula and put in an air-tight screw cap vial for future uses.

FESEM analysis, DLS and zeta potential analysis were conducted for the coated iron oxide nanoparticles as well. The results and discussions obtained have been discussed in the forthcoming chapter.

3.2.6 Anti-microbial activity and protein adsorption test of coated nanoparticles

Agar medium was prepared for culturing E-Coli. In 100 ml of water, 2.5 g of Luria Bertani Broth was added, then 3 g of agar was added to the above solution. The solution was mixed thoroughly and was autoclaved at 121°C for 15mins.

Under Laminar air flow hood, 20 ml of autoclaved media was poured onto each of three petriplates. The petriplates were left undisturbed for 10-15 mins until agar was solidified.

3 equidistant wells were carefully cut out in the solidified media. One well was left for positive control and 500µl of metrinidazole drug (1mg/ml) was added to it. In the other two wells, 500µl of coated and uncoated iron oxide nanoparticles of concentration 1mg/ml were poured. 1ml of E-Coli culture was added in the centre of the petriplates and spread evenly with an autoclaved L-shaped rod. The petriplates were wrapped tightly with parafilm and labelled properly. The inoculated petriplates were kept in an incubator at 35°C overnight. On the following day, petridishes were inspected for zones of inhibition.

10 mg of dried iron oxide nanoparticles and chitosan coated iron oxide nanoparticles were taken in two different test tubes. In each test tube 10 ml of BSA solution was added. In one separate test tube 10 ml of BSA solution was added. The mixture was kept in a shaker operating at 200 rpm for 10 to 240 minutes each. After 6 hours, 12 hours, 18 hours, and 24 hours, each test tube was centrifuged and 1 ml of solution was taken from the supernatant of each test tube and analyzed using spectrophotometer at 595nm. Analysis was done by Bradford assay of protein solution.

100 µl of the protein samples and blank was taken in different test tubes. 1ml of Bradford reagent was added in each test tube. It was then diluted with 2ml of water. All the test tubes were incubated in dark for 15 minutes. Optical density of the samples was measured at 595 nm using spectrophotometer. Then the graph was plotted according to the data obtained.

3.2.7 Analysis of arsenic removal from water

A solution of 0.1M concentration was prepared by dissolving arsenic trioxide in distilled water. A single drop of concentrated hydrochloric acid was added to the solution to aid the dissolution of arsenic trioxide in water. The beaker was kept on a magnetic stirrer. The temperature of the stirrer was set to 45°C to slightly warm the solution so that the arsenic trioxide dissolves uniformly without forming lumps. The solution was kept on the magnetic stirrer for 2-2.5hours and then left undisturbed for 15mins. This solution was used as the stock solution for the arsenic removal studies.

6 solutions containing 120ppm, 140ppm, 160ppm, 180ppm, 200ppm and 220ppm of arsenic trioxide in distilled water were prepared from the stock solution. Absorbance for all the 6 solutions was checked at 220.4nm and the data obtained was used to plot a standard curve. The standard curve was plotted using Origin software and the graph obtained was fitted linearly.

Two suspensions, one containing 10ppm of chitosan coated iron oxide nanoparticles and the other containing 100ppm of iron oxide nanoparticles, were prepared in distilled water. The suspensions were sonicated for 9-12mins so as to disperse the nanoparticles evenly in the water. 1ml of each of the two suspensions was added to 10ml of the 0.1M stock arsenic trioxide solution prepared initially. This mixture was left undisturbed for about 2-3 hours, allowing the coated nanoparticles to interact with the arsenic trioxide particles present in the suspension.

The absorbance of these two suspensions was measured using a UV Spectrophotometer at 220.4nm. The results obtained have been discussed in the forthcoming chapter.

CHAPTER 4:
RESULTS AND DISCUSSIONS

Iron oxide nanoparticles were synthesized by an optimized electrochemical method and were subsequently coated with chitosan for modifying the surface properties of the nanoparticles. The morphological characterization of the uncoated and coated nanoparticles were carried out using XRD, FESEM, DLS and Zeta Potential analysis and the results obtained are discussed in the current chapter.

4.1 Dynamic Light Scattering

Initially, seven samples obtained from the electrochemical synthesis procedure were analysed for the particle size distribution present in them. The intensity of the size distribution patterns are given below.

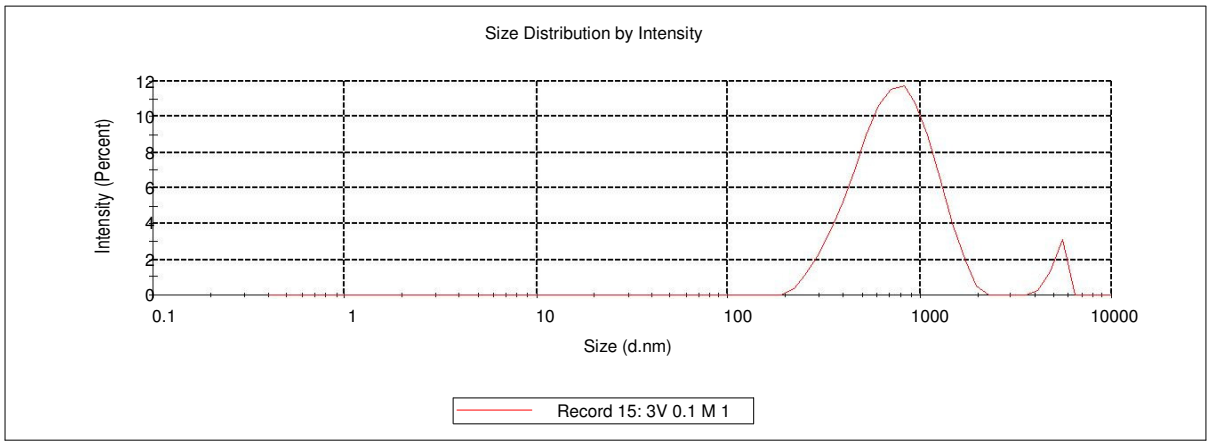

Fig 3: Size vs. Intensity data obtained from DLS for 0.1M LiCl, 3V, 15min

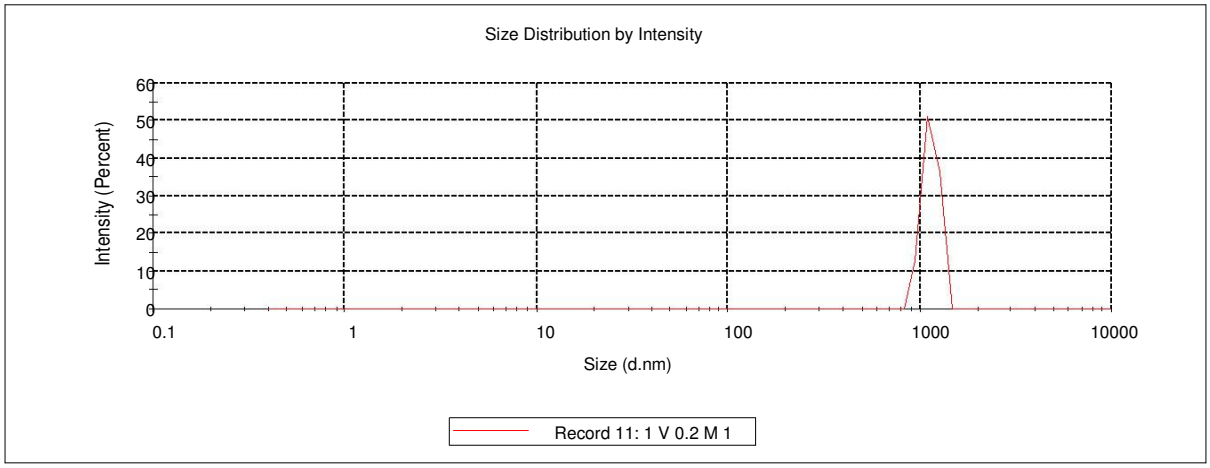

Fig 4: Size vs. Intensity data obtained from DLS for 0.2M LiCl, 1V, 15min

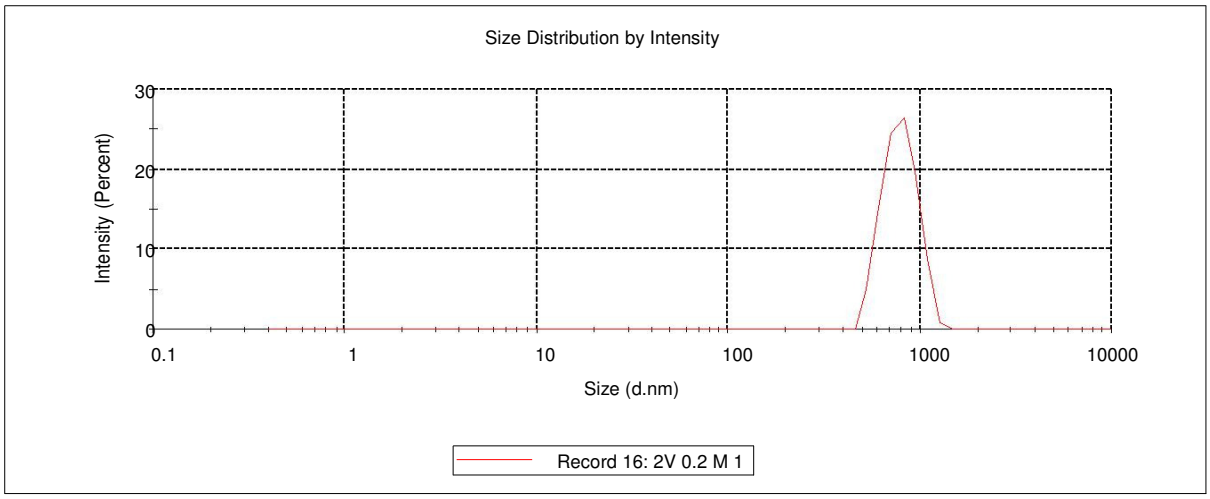

Fig 5: Size vs. Intensity data obtained from DLS for 0.2M LiCl, 2V, 15min

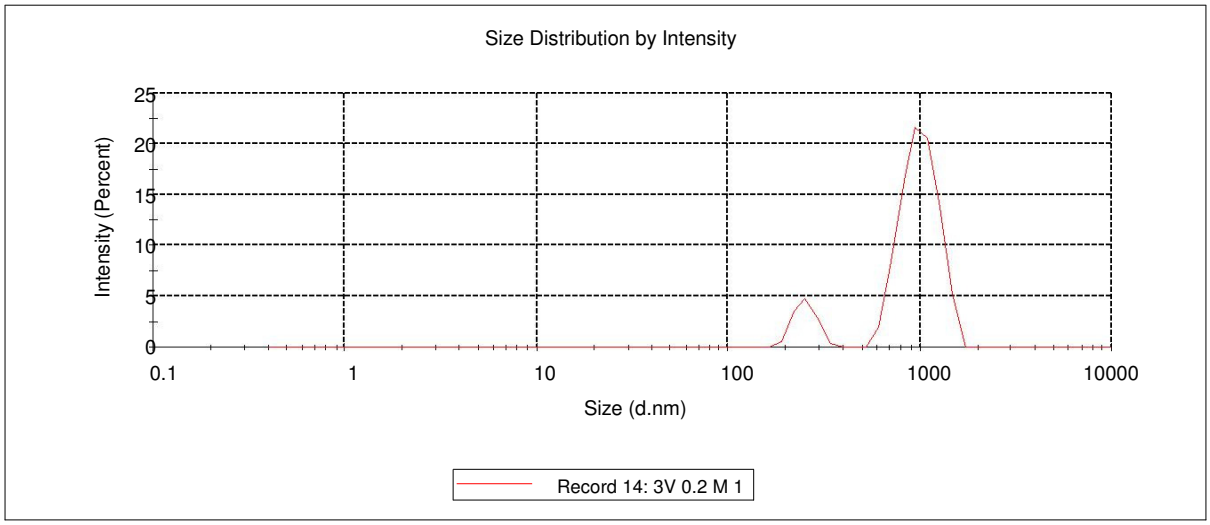

Fig 6: Size vs. Intensity data obtained from DLS for 0.2M LiCl, 3V, 15min

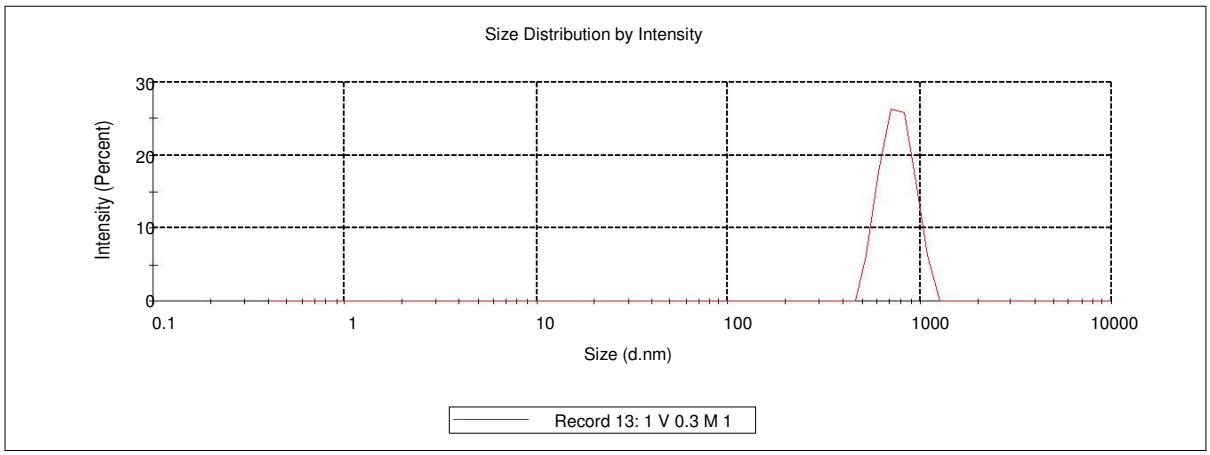

Fig 7: Size vs. Intensity data obtained from DLS for 0.3M LiCl, 1V, 15min

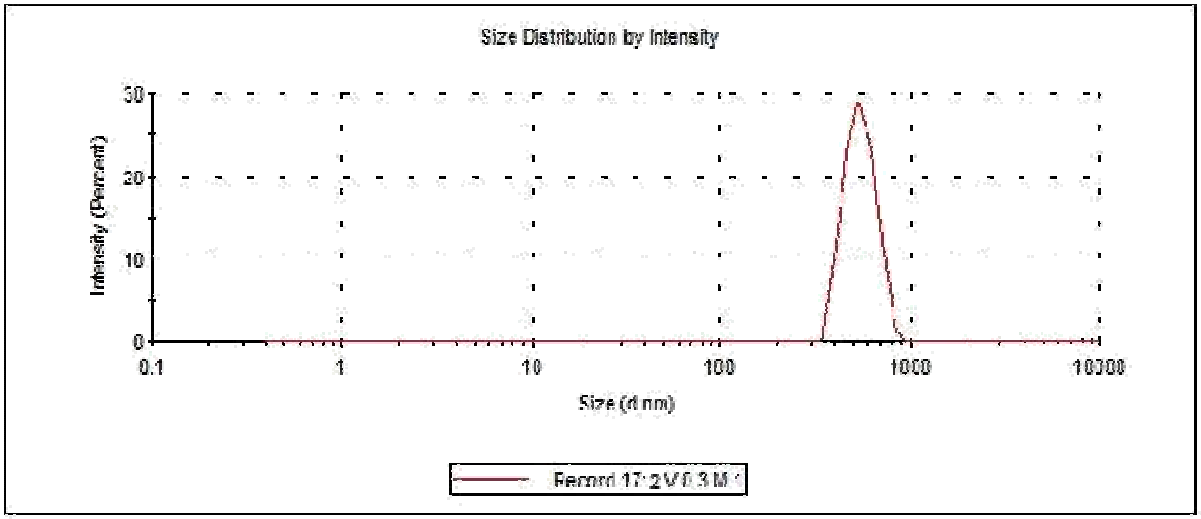

Fig 8: Size vs. Intensity data obtained from DLS for 0.3M LiCl, 2V, 15min

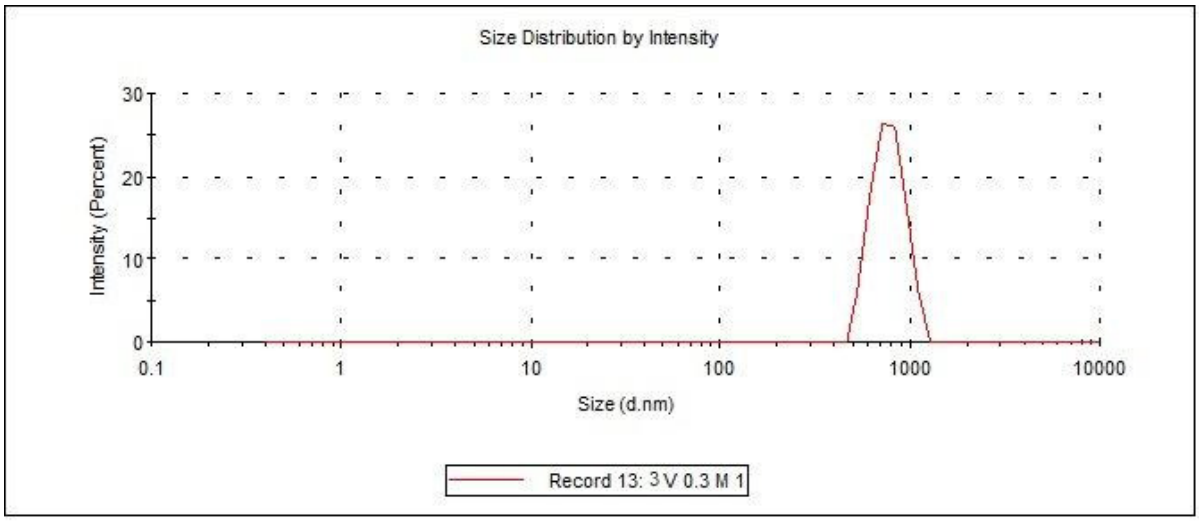

Fig 9: Size vs. Intensity data obtained from DLS for 0.3M LiCl, 3V, 15min

The size distribution patterns obtained were carefully analysed and samples were screened based on the sizes of the nanoparticles present in the samples. The following table gives the size of nanoparticles and their intensities in each of the seven samples. The samples showing the smallest clusters of nanoparticles were chosen for further analysis. Based on the DLS data, the minimum size distribution was obtained at process parameters 0.3M 2V and 0.3M 3V.

Table 1: Size distribution measurement of the nanoparticles by DLS

Working Parameters	Size (d.nm)	% Intensity	Standard Deviation (d.nm)
0.1 M, 3V			
Peak 1	795.2	95.4	344.9
Peak 2	5275	4.6	425.4
0.2 M, 1V	1151	100.0	109.9
0.2 M, 2V	805.0	100.0	159.6
0.2M, 3V			
Peak 1	1018	88.0	214.5
Peak 2	255.1	12.0	34.12
0.3 M, 1V	779.2	100.0	149.5
0.3M, 2V	546.5	100.0	99.61
0.3 M, 3V	723.2	100.0	119.1

Samples prepared at 0.3M 2V and 0.3M 3V were selected as better samples compared with the other samples taken under the experimental processing condition. The iron oxide nanoparticles were synthesized by the optimized experimental conditions. They were washed with ethanol to remove LiCl traces and then dried carefully. The nanoparticles were dispersed in distilled water and sonicated for 9-12mins prior to subjecting them for DLS. The size distribution graphs obtained are shown below.

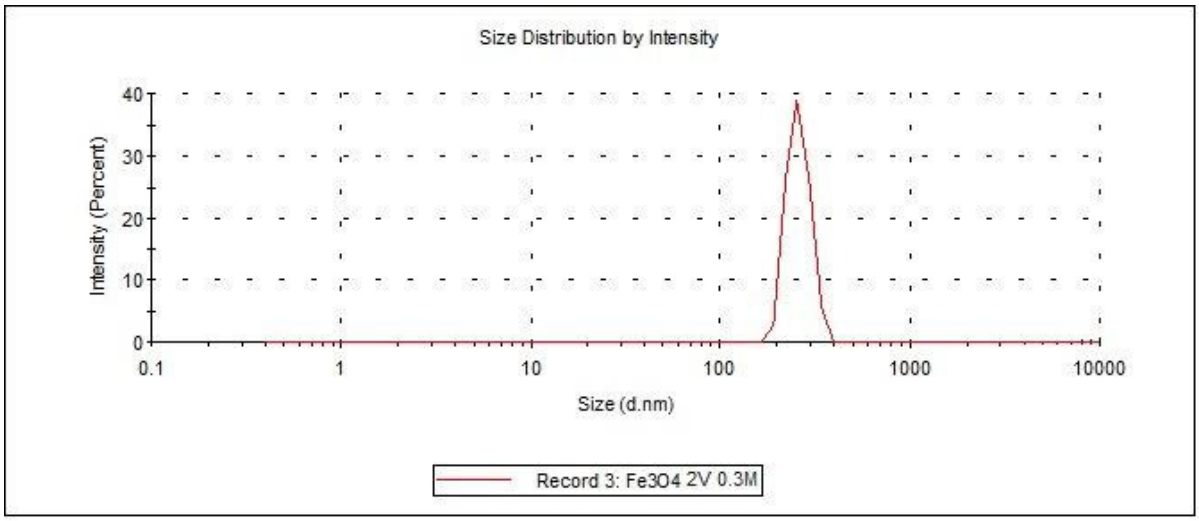

Fig 10: Size vs. Intensity data obtained from DLS for 0.3M LiCl, 2V, 30mins (ethanol washed samples)

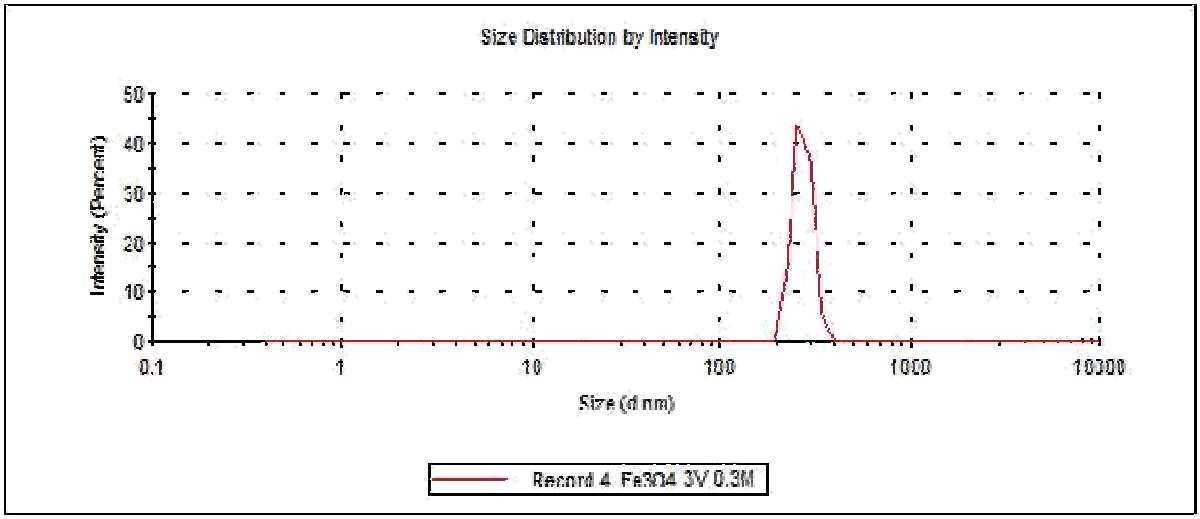

Fig 11: Size vs. Intensity data obtained from DLS for 0.3M LiCl, 3V, 30mins

Table 2: Size distribution measurement of the screened nanoparticles by DLS

Working Parameters (peak 1)	Size(d.nm)	% Intensity	Standard Deviation (d.nm)
0.3 M, 2 V	259.0	100.0	35.57
0.3 M, 3V	270.1	100.0	31.01

Thus, it was found that the nanoparticles had a size distribution ranging from 150-250nm which was less than the previously obtained size distribution. This can be attributed to the removal of LiCl traces by proper ethanol washing. The size measured by DLS is not of the individual nanoparticles but the agglomerates formed by them. The principle reason behind this is that iron oxide nanoparticles have hydrophobic surfaces with a large surface area-to-volume ratio. Hydrophobic interactions between the nanoparticles due to absence of any kind of coating leads to them forming large agglomerates, thus showing a significant increase in particle size during analyses. (31)

4.2 Field Emission Scanning Electron Microscopy

FESEM was carried out for the two screened samples – 0.3M 2V and 0.3M 3V. The figures below show the morphological characteristics of the two samples.

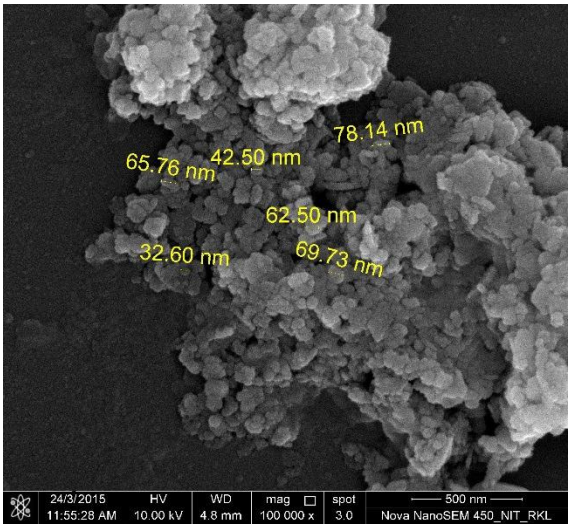

(a)

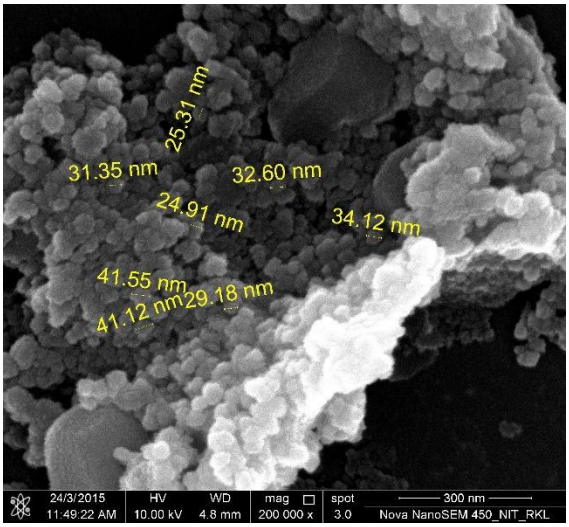

(b)

Fig 12: FESEM images of Fe_3O_4 nanoparticles synthesized by electrochmical method (0.3M, 2V) under different magnifications : a) 100k x and b) 200k x.

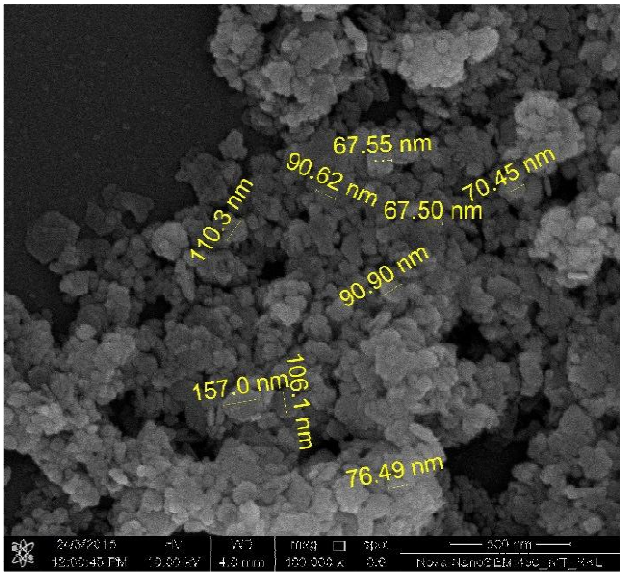

Fig 13: FESEM images of Fe_3O_4 nanoparticles synthesized by electrochmical method (0.3M, 3V) at 100k x magnification

From the FESEM data, it was observed that the particle size in the sample of 0.3M LiCl operated at 3V was much bigger than the particle size in the sample of 0.3M LiCl operated at 2V. Thus, the work was proceeded with the sample having the process parameters of 0.3M 2V sample.

4.3 Zeta Potential

Uncoated iron oxide nanoparticles from 0.3M 2V showed a stable zeta potential which was below the standard -25V, showing that the nanoparticles formed were of a stable nature.

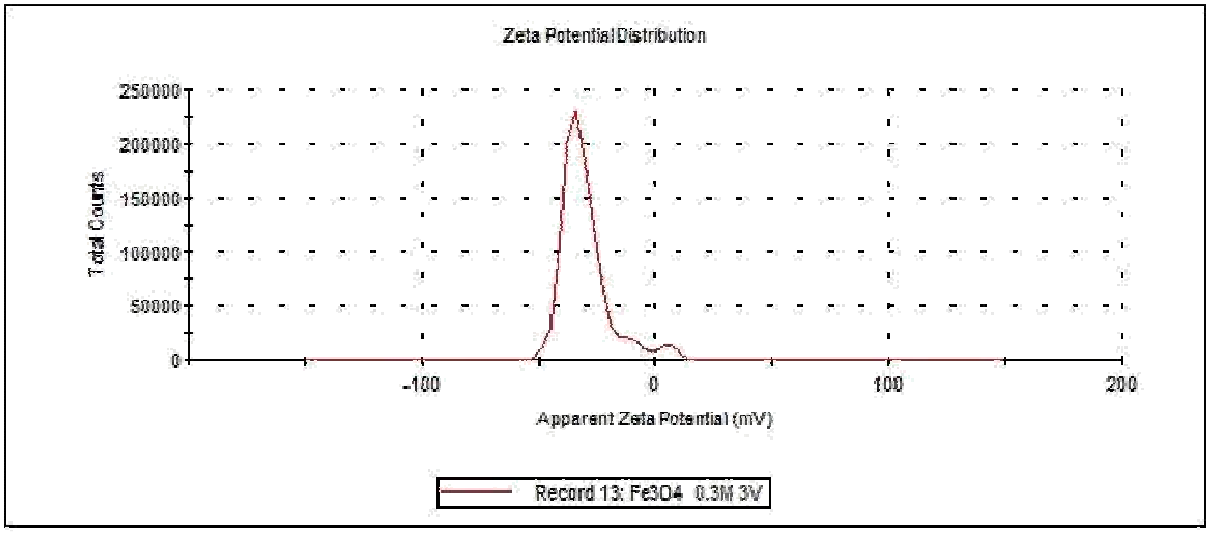

Fig 14: Zeta Potential distribution for 0.3M 3V

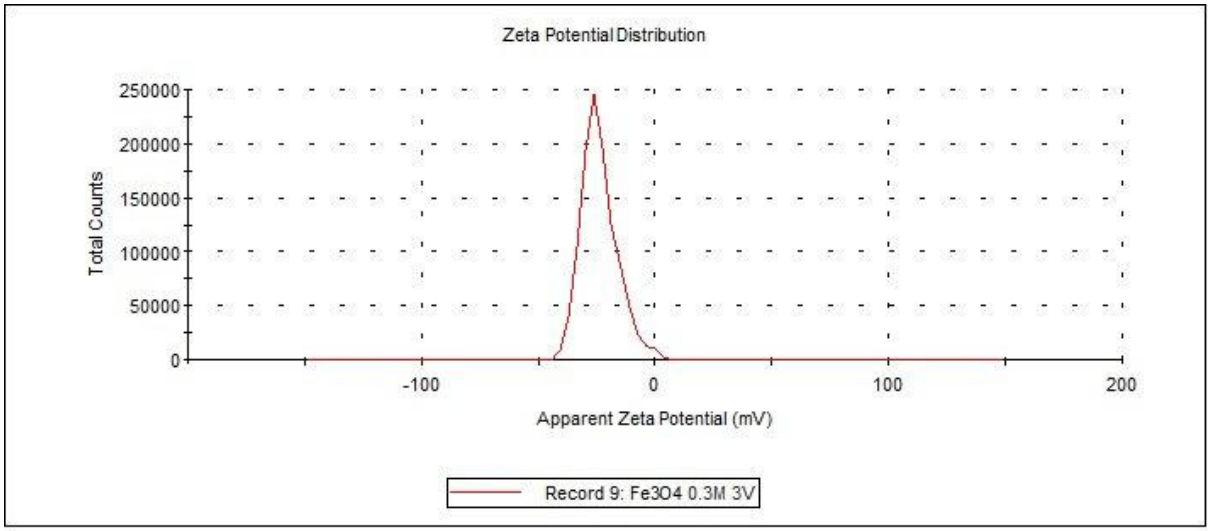

Fig 15: Zeta Potential distribution for 0.3M 3V

Table 3: Zeta Potential distribution analysis

Working Parameters (peak 1)	Voltage (mV)	% Intensity	Standard Deviation (d.nm)
0.3 M, 2 V	-32.7	89.8	6.73
0.3 M, 3 V	-23.8	100.0	7.78

The iron oxide nanoparticles from the sample with parameters 0.3M 3V showed a zeta potential value which was negative but less negative than the standard value of -25V.

After the FESEM and Zeta Potential analysis, we proceeded with only one single sample for coating procedures.

4.4 Characterization and comparison of chitosan coated nanoparticles

Coating of nanoparticles was undertaken only for the nanoparticles obtained from the 0.2M 2V sample. The particle size analysis for these coated particles was done with DLS and gave the graph as shown below.

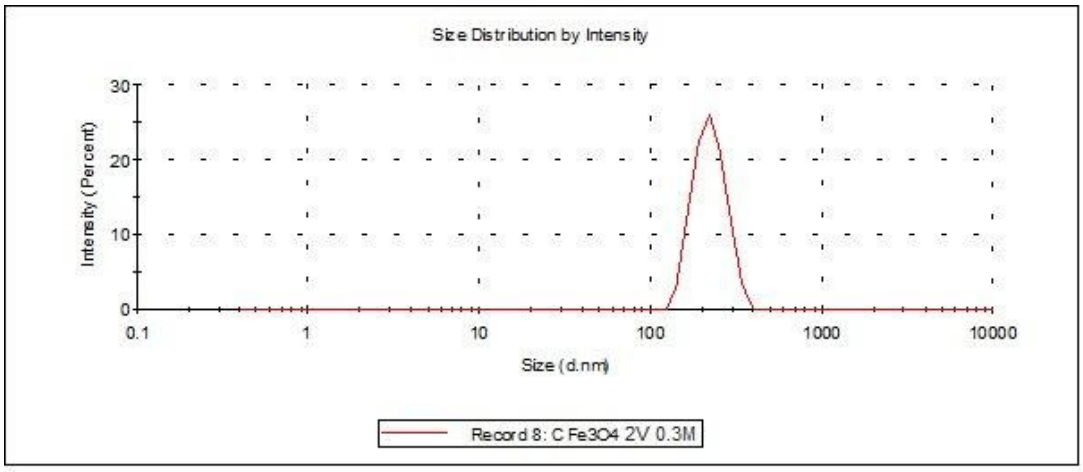

Fig 16: Size vs. Intensity data obtained from DLS for chitosan coated nanoparticles with process parameters 2V, 0.3M

Table 4: Size distribution measurement of the chitosan coated nanoparticles by DLS

Working Parameters (peak 1)	Size (d.nm)	% Intensity	Standard Deviation (d.nm)
0.3 M, 2 V	300.3	100.0	47.03

The particle sizes were found to be larger than the ones obtained in the DLS of the uncoated samples, confirming the coating of the nanoparticles.

Characterization of the chitosan coated nanoparticles was conducted using FESEM also. The size obtained was found to be slightly larger than the values of the uncoated nanoparticles, indicating a near uniform coating of the nanoparticles with chitosan.

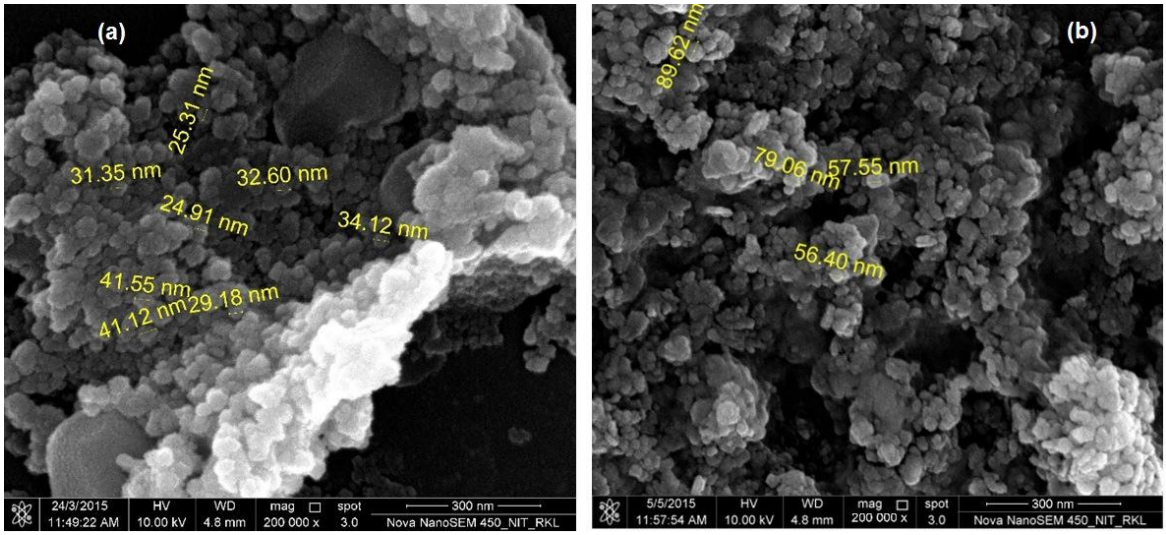

Fig 17: FESEM images of Fe_3O_4 nanoparticles with process parameters 0.3M, 2V in (a) uncoated and (b) coated conditions at 200k x magnification.

Zeta potential analysis of the coated samples showed a potential that was greater than +25V which confirmed that the nanoparticles were uniformly coated and were stable.

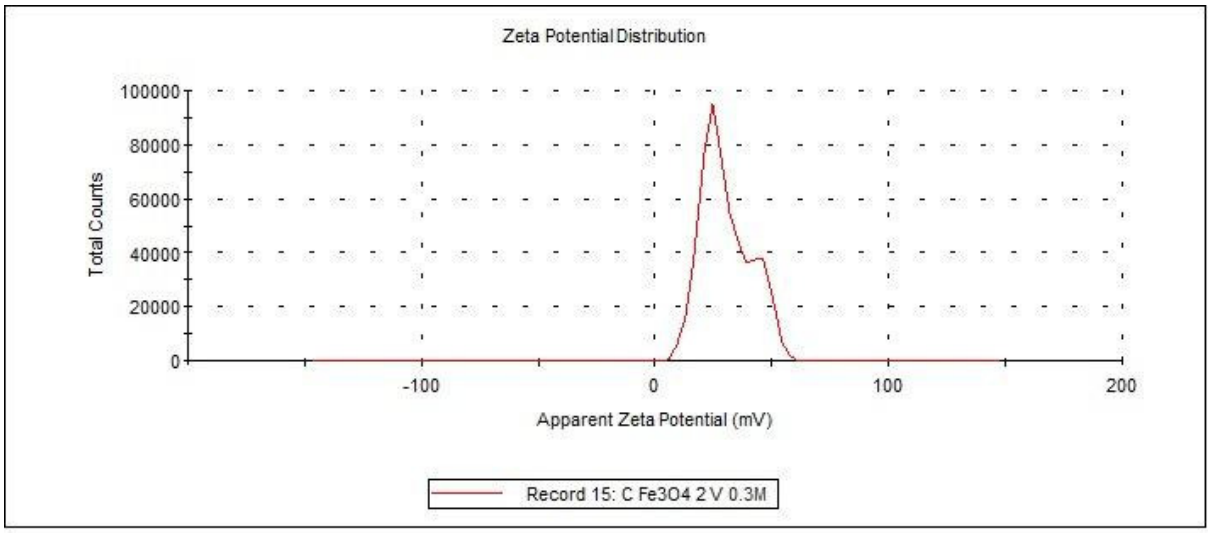

Fig 18: Zeta potential distribution for coated sample

Table 5: Zeta Potential distribution for coated samples

Working Parameters	Mean (mV)	Area (%)	Standard Deviation (mV)
0.3 M, 2 V Peak 1 Peak 2	 26.4 44.9	 75.7 24.3	 7.13 4.57

4.5 X-Ray Diffraction analysis

X-ray diffraction analysis showed the presence of Fe_3O_4 particles with traces of Fe_2O_3 particles in the samples prepared. The peaks obtained were compared and matched with the available standard data.

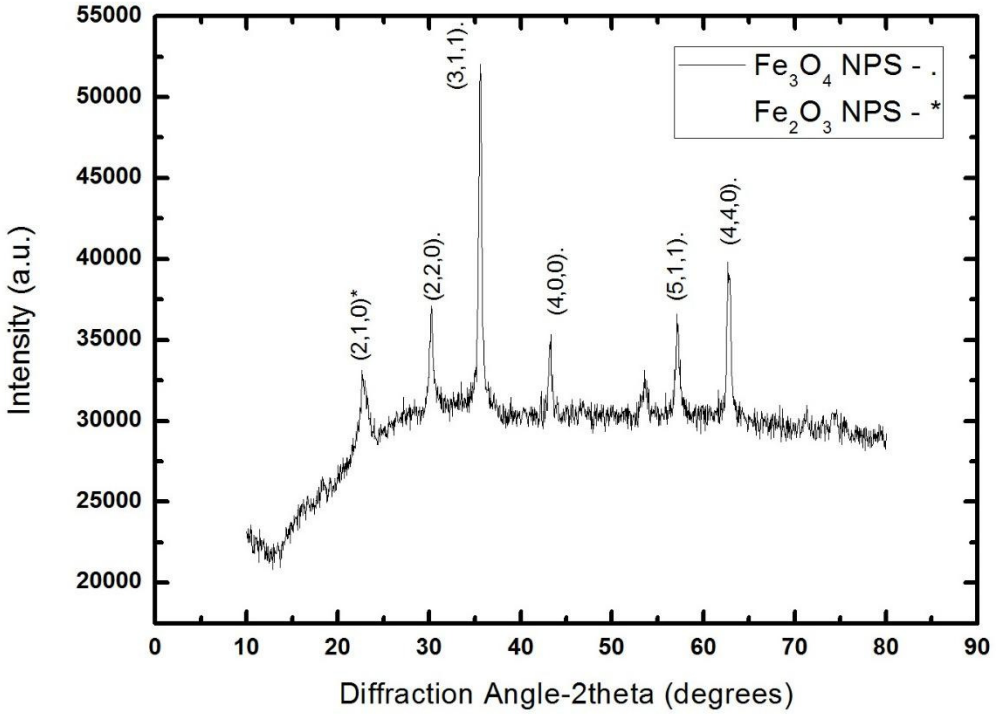

Fig 19: XRD pattern of Fe_3O_4 nanoparticles for 2V, 0.2M

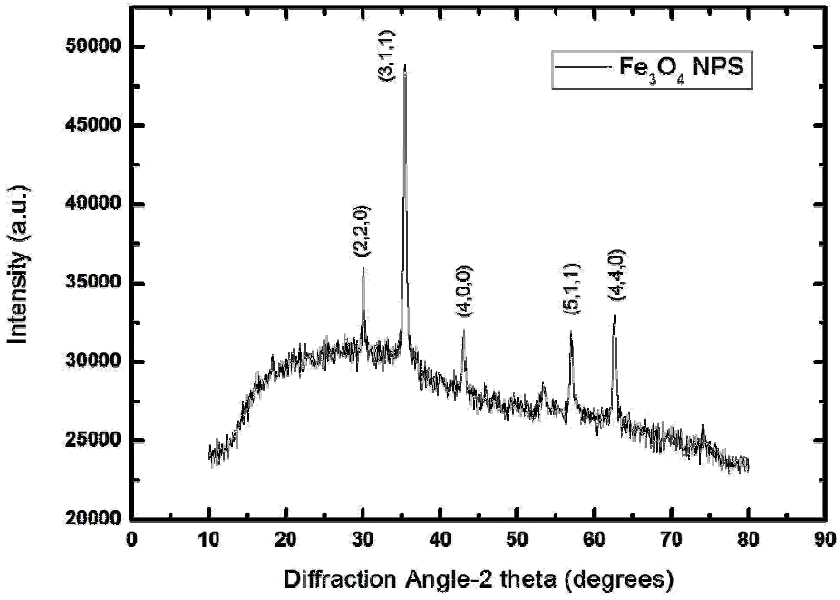

Fig 20: XRD pattern of Fe_3O_4 nanoparticles for 0.3M, 1V

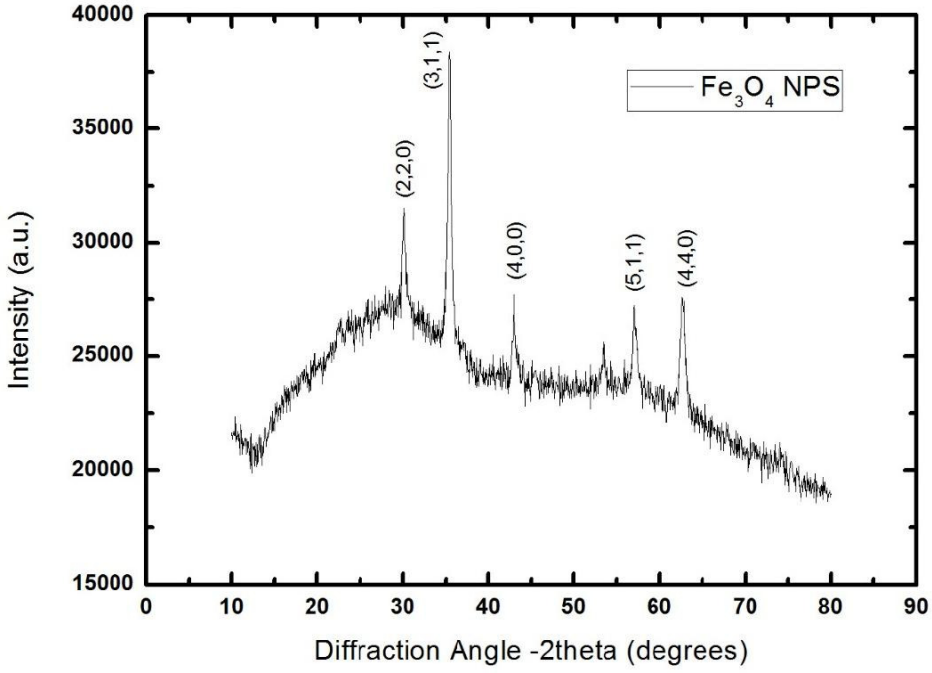

Fig 21: XRD pattern of Fe_3O_4 nanoparticles for 0.3M, 2V

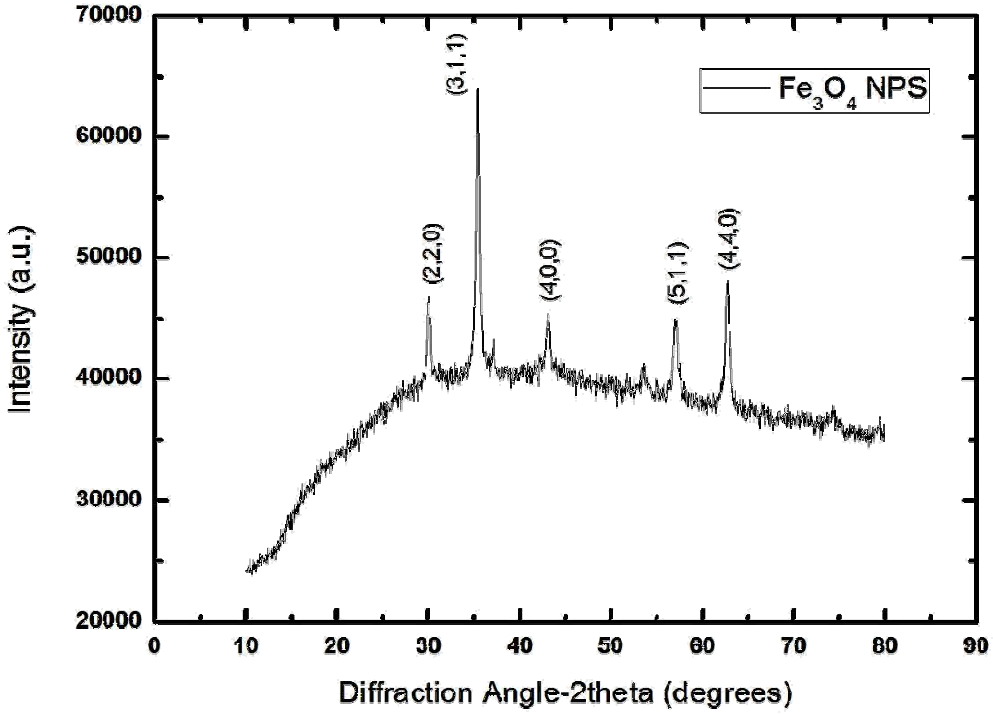

Fig 22: XRD pattern of Fe_3O_4 nanoparticles for 0.3M, 3V

4.6 Arsenic removal from water using chitosan coated iron oxide nanoparticles

The standard curve for arsenic trioxide was plotted by measuring the optical density of the solution at various concentrations viz., 120ppm, 140ppm, 160ppm, 180ppm, 200ppm, 220ppm, which were all prepared from a 0.1M solution of As_2O_3 in distilled water under slight acidic conditions. The absorbance was measured at a wavelength of 220.4nm. The maximum wavelength for As_2O_3 absorbance was determined by checking the absorbance of the 0.1M solution from 200-300nm (34). The peak showed at 220.4nm and thus this was the wavelength

at which the OD was measured for the other relevant data. The standard curve obtained is given below.

Table 6: OD data obtained at 220.4nm

Conc. Of As2O3 in ppm	OD at 220.4nm
120	0.0015
140	0.0018
160	0.0019
180	0.0023
200	0.0025
220	0.0029

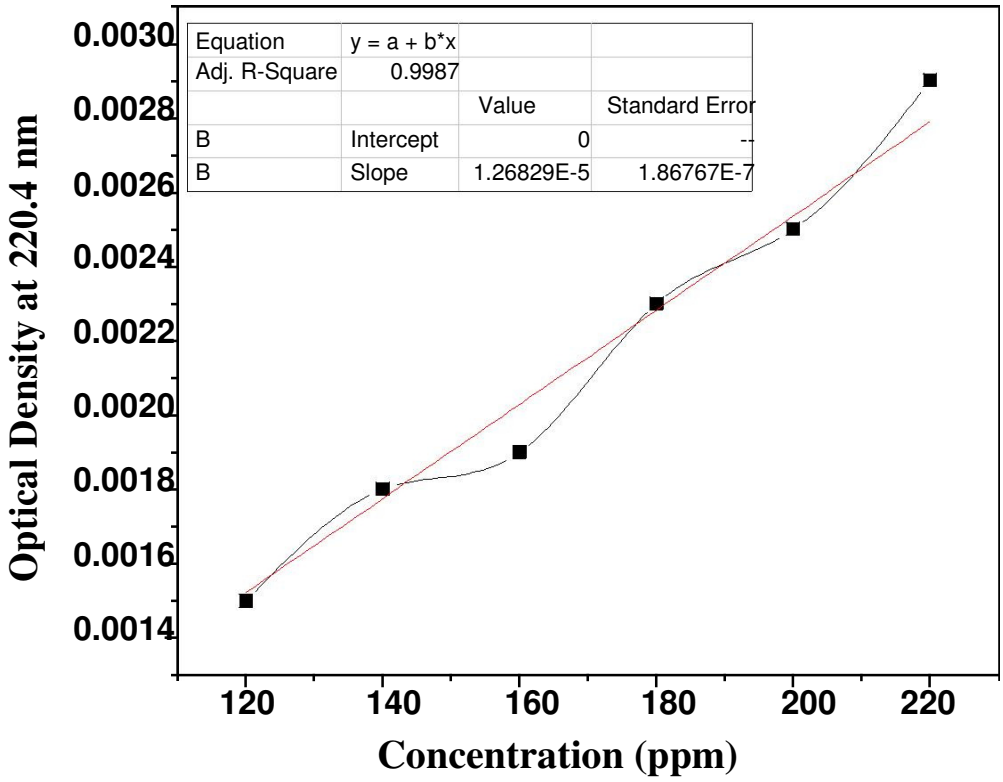

Fig 23: Standard curve for As_2O_3

1ml of each of the two suspensions of 10ppm and 100ppm iron oxide nanoparticles was added to 10ml of the 0.1M stock arsenic trioxide solution prepared initially. The absorbance of these two suspensions was measured using a UV Spectrophotometer at 220.4nm. It was observed

that the absorbance of the samples having iron oxide nanoparticles was lower than the absorbance of the sample without the nanoparticles. This shows that some of the As_2O_3 particles were removed after interaction with the chitosan coated iron oxide nanoparticles.

Table 7: Reduction of As_2O_3 concentration after addition of coated iron oxide nanoparticles

	Concentrations	OD at 220.4nm	ppm present initially	ppm reduced after addition of coated nps
solution	0.1 M	1.27	100157.7287	(Original Solution)
nps	100 ppm	1.197	94400.63091	5757.097792
nps	10 ppm	1.213	95662.46057	4495.268139

4.7Anti-microbial activity of uncoated and coated nanoparticles

After analysis of Anti-microbial activity of uncoated and coated nanoparticles it was found that anti-microbial activity of the drug metronidazole is highest. It was also found that chitosan coated nanoparticles show more anti-microbial activity than uncoated nanoparticles. This proved that efficiency of coated nanoparticles is more than that of uncoated nanoparticles.

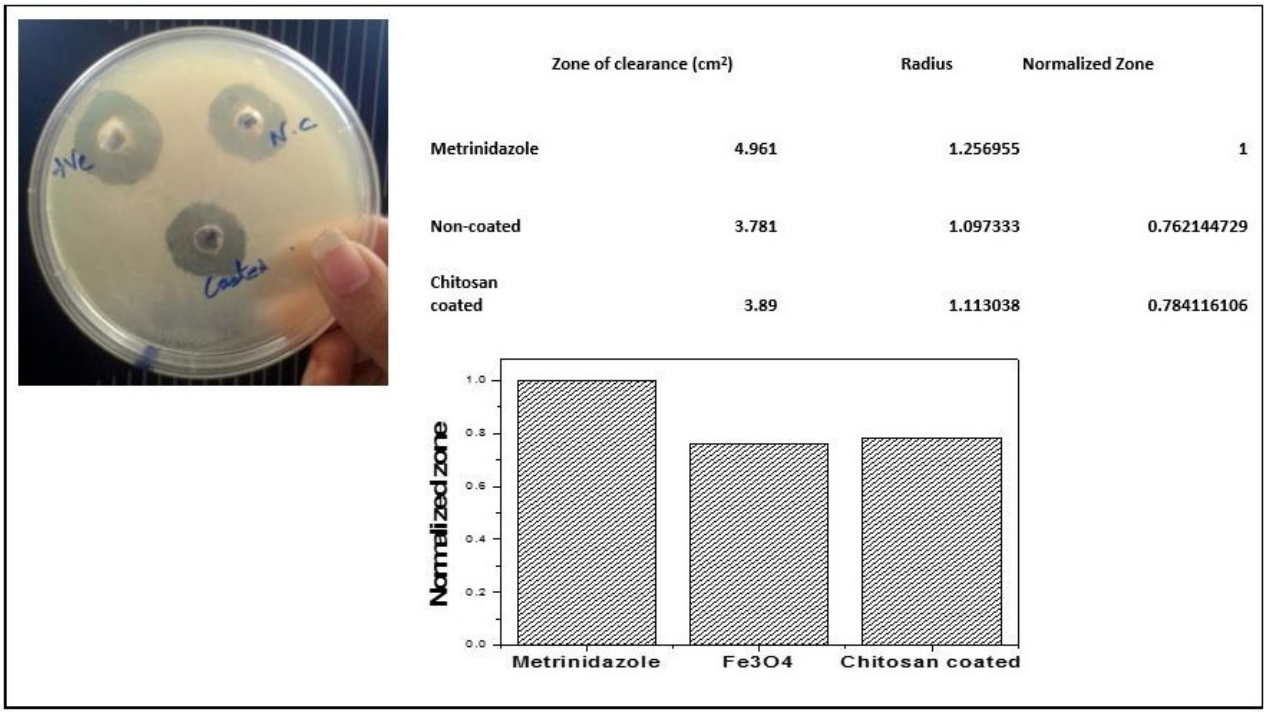

Fig 24: Anti-microbial activity

4.8 Protein adsorption

After analysis of the results, it was found that protein adsorption by chitosan coated iron oxide nanoparticles is more than that of uncoated nanoparticles. Thus it shows that chitosan coated iron oxide nanoparticles are more efficient than uncoated nanoparticles.

Table 8: Standard values for protein adsorption taken with BSA

BSA solution (OD)	BSA solution (Protein Conc.)
0.915	989.7241752
0.892	964.8458626
0.9	973.4991888
Average	976.0230755
Standard deviation	12.62973131
0.91	984.3158464
0.89	962.6825311
0.92	995.1325041
Average	980.7102939
Standard deviation	16.52271749
0.92	995.1325041
0.9	973.4991888
0.92	995.1325041
Average	987.921399
Standard deviation	10.19804263
0.89	962.6825311
0.87	941.0492158
0.88	951.8658734
Average	951.8658734
Standard deviation	8.831763991

Table 9: OD values for uncoated nanoparticles

Uncoated Fe3O4 nps OD	Uncoated Fe3O4 nps (Protein Conc.)
0.856	925.9058951
0.845	914.0075717
0.871	942.1308816
Average	927.3481161
Standard deviation	14.11701601
0.75	811.249324
0.73	789.6160087
0.73	789.6160087
Average	796.8271138
Standard deviation	12.49000042
0.68	735.5327204
0.67	724.7160627
0.66	713.8994051
Average	724.7160627
Standard deviation	8.831763991
0.62	670.6327745
0.6	648.9994592
0.58	627.3661439
Average	648.9994592
Standard deviation	17.66352798

Table 10: OD values for coated nanoparticles

Coated Fe_3O_4 nps OD	Coated Fe_3O_4 nps (Protein Conc.)
0.842	910.7625744
0.85	919.4159005
0.867	937.8042185
Average	922.6608978
Standard deviation	13.80978403
0.68	735.5327204
0.69	746.349378
0.7	757.1660357
Average	746.349378
Standard deviation	10.81665765
0.42	454.2996214
0.47	508.3829097
0.45	486.7495944
Average	483.1440418
Standard deviation	22.22611863
0.33	356.9497025
0.38	411.0329908
0.32	346.1330449
Average	371.3719127
Standard deviation	28.39014918

CHAPTER 5:

CONCLUSION AND FUTURE SCOPE

5.1 Conclusion

The electrochemical synthesis process of synthesizing iron oxide nanoparticles was optimized in this study. It was found that the production of Fe_3O_4 or Fe_2O_3 nanoparticles depended on the voltage being applied and the concentration of the electrolytic bath. The study aimed at the synthesis of Fe_3O_4 nanoparticles. It was found that increasing the time of the electrochemical process beyond 30mins resulted in the deposition of impurities in the solution. Nanoparticles were obtained in a uniform size distribution in the process with parameters 0.3M LiCl operated at 2V. The average approximate nanoparticle size obtained was 58.54nm. The nanoparticles thus synthesized were coated with chitosan. Characterization was carried out for determination of the morphological and physical characteristics of the coated and uncoated Fe_3O_4 nanoparticles. The utility of the chitosan coated Fe_3O_4 nanoparticles was analysed by using them for the removal of As_2O_3 from water. The anti-microbial activity and protein adsorption capacity of the chitosan coated Fe_3O_4 nanoparticles was also successfully analysed and recorded.

5.2 Future Scope

The electrochemical synthesis method that was optimized in the current study is a cost-effective and simple method for the synthesis of Fe_3O_4 nanoparticles under laboratory conditions. Further optimization of the process can be undertaken to scale up the process for production of larger amounts of Fe_3O_4 nanoparticles. Chitosan coated Fe_3O_4 nanoparticles are seen to be effective in removal of arsenic trioxide from water. This can be used for cost-effective treatment of waste water and industrial effluents which contain arsenic at very high levels and are often responsible for groundwater contamination. The application of chitosan coated Fe_3O_4 nanoparticles in anti-microbial activities and protein adsorption can be successfully used for tissue engineering purposes.

CHAPTER 6:
REFERENCES

References

1. R.M. Cornell, U. Schwertmann, The Iron Oxides. Structure, Properties, Reaction, Occurrence and Uses, VCH, Germany and USA, 1996.
2. R.M. Cornell, U. Schwertmann, The Iron Oxides: Structure, Properties, Reactions, Occurrences and Uses, Wiley.com, 2003.
3. Starowicz, Maria et al. "Electrochemical Synthesis of Magnetic Iron Oxide Nanoparticles with Controlled Size." Journal of Nanoparticle Research 13.12 (2011): 7167–7176. PMC. Web. 4 Dec. 2014.
4. Catherine C Berry, Adam S G Curtis." Functionalisation of magnetic nanoparticles for applications in biomedicine." 18 June 2003
5. Susheel Kalia, Sarita Kango, Amit Kumar, Yuvaraj Haldorai, Bandna Kumari, Rajesh Kumar; "Magnetic polymer nanocomposites for environmental and biomedical applications"; 8 August 2014.
6. Coey JMD (1999) Whither magnetic materials? J Magn Magn Mater 196–197:1–7.
7. Shull RD, Bennett LH (1992) Nanocomposite magnetic materials. Nanostruct Mater 1:83–88
8. Lu A-H, SchmidtW, Matoussevitch N, Bonnemann HB, Spliethoff B, Tesche B, Bill E, KieferW, Schuth F (2004) Nanoengineering of a magnetically separable hydrogenation. Angew Chem Int Ed 43:4303–4306
9. Zhu J, Wei S, Chen M, Gu H, Rapole SB, Pallavkar S, Ho TC, Hopper J, Guo Z (2013)Magnetic nanocomposites for environmental remediation. Adv Powder Technol 24:459–467.
10. Gupta S, Ranjit R, Mitra C, Raychaudhuri P, Pinto R (2001) Enhanced room-temperature magnetoresistance in La0.7 Sr0.3 MnO3-glass composites. Appl Phys Lett 78:362–364

11. Huang Y-H, Chen X, Wang Z-M, Liao C-S, Yan C-H, Zhao H-W, Shen B-G (2002) Enhanced magnetoresistance in granular La2/3Ca1/3MnO3/polymer composites. J Appl Phys 91:7733–7735.

12. Lu A-H, Salabas EL, Schuth F (2007) Magnetic nanoparticles: synthesis, protection, functionalization, and application. Angew Chem Int Ed 46:1222–1244.

13. Kango S, Kalia S, Celli A, Njuguna J, Habibi Y, Kumar R (2013) Surface modification of inorganic nanoparticles for development of organic–inorganic nanocomposites—a review. Prog Polym Sci 38: 1232–1261

14. Tai Y, Wang L, Yan G, Gao J-M, Yu H, Zhang L (2011) Recent research progress on the preparation and application of magnetic nanospheres. Polym Int 60:976–99

15. Berry CC, Curtis ASG. Functionalisation of magnetic nanoparticles for applications in biomedicine. J Phys D: Appl Phys 2003; 36:R198–206.

16. Tartaj P, Morales MP, Veintemillas-Verdaguer S, Gonza´ lez-Carren˜ o T, Serna CJ. The preparation of magnetic nanoparticles for applications in biomedicine. J Phys D: Appl Phys 2003;36:R182–97.

17. Chatterjee J, Haik Y, Chen C-J. Size dependent magnetic properties of iron oxide nanoparticles. J Magn Magn Mater 2003;257(1):113–8.

18. C.C. Berry, S. Wells, S. Charles, A.S.G. Curtis, Dextran and albumin derivatised iron oxide nanoparticles: influence on fibroblasts in vitro, Biomaterials 24 (2003) 4551–4557.

19. J. Ren, H.Y. Hong, T.B. Ren, X.R. Teng, Preparation and characterization of magnetic PLA–PEG composite nanoparticles for drug targeting, React. Funct. Polym. 66 (2006) 944–951.

20. Y. Zhang, J. Zhang, Surface modification of monodisperse magnetite nanoparticles for improved intracellular uptake to breast cancer cells, J. Colloid Interface Sci. 283 (2005) 352–357.

21. S. Laurent, D. Forge, M. Port, A. Roch, C. Robic, L.V. Elst, R.N. Muller, Magnetic iron oxide nanoparticles: synthesis, stabilization, vectorization, physicochemical characterizations, and biological applications, Chem. Rev. 108 (2008) 2064–2110.

22. Y. Hu, Y. Ding, D. Ding, M.J. Sun, L.Y. Zhang, X.Q. Jiang, C.Z. Yang, Hollow chitosan/poly(acrylic acid) nanospheres as drug carriers, Biomacromolecules 8 (2007) 1069–1076.

23. T.Y. Guo, Y.Q. Xia, J. Wang, M.D. Song, B.H. Zhang, Chitosan beads as molecularly imprinted polymer matrix for selective separation of proteins, Biomaterials 26 (2005) 5737–5745.

24. Gui-yin Li a,b, Yu-ren Jiang b,., Ke-long Huangb, Ping Ding b, Jie Chenb," Preparation and properties of magnetic Fe3O4–chitosan nanoparticles"; Published on 7 January 2008.

25. Boyer C, Whittaker MR, Bulmus V, Liu J, Davis TP. The design and utility of polymerstabilized iron oxide nanoparticles for nanomedicine applications. NPG Asia Mater 2010; 2:23–30.

26. Gupta AK, Gupta M. Synthesis and surface engineering of iron oxide nanoparticles for biomedical applications. Biomaterials 2005a; 26:3995–4021.

27. M. Morales, Veintemillas-Verdaguer S., Montero M. I., Serna C.J., Surface and internal spin canting in γ-Fe2O3 nanoparticles, Chem. Mater.11(11)(1999)3058–3064.

28. Anderson S. A., Rader R. K., Westlin W. F., Null C., Jackson D., Lanza G. M., Wickline S. A., Kotyk J. J., Magnetic resonance contrast enhancement of neovasculature with $\alpha v\beta 3$-targeted nanoparticles, Magn.Reson.Med.44 (3) (2000) 433-439.

29. Mahmoudi M., Simchi A., Milani A. S., Stroeve P., Cell toxicity of super-paramagnetic iron oxide nanoparticles, J.Colloid Interface Sci.336 (2) (2009) 510-518.

30. Maliar T., Electrochemical aspects of the synthesis of iron particles, Mater.Sci.18 (2012) 3.

31. Wu W., Quangua H., Jiang C., Magnetic Iron Oxide Nanoparticles: Synthesis and Surface Functionalization Strategies, Nanoscale Research Letters 2008, 3:397-415

32. Qu, J., Liu, G., Wang, Y., & Hong, R. (2010). Preparation of Fe 3 O 4–chitosan nanoparticles used for hyperthermia. Advanced Powder Technology, 21(4), 461-467.

33. Mai, T. T. T., Ha, P. T., Pham, H. N., Le, T. T. H., Pham, H. L., Phan, T. B. H., & Nguyen, X. P. (2012). Chitosan and O-carboxymethyl chitosan modified Fe_3O_4 for hyperthermic treatment. Advances in Natural Sciences: Nanoscience and Nanotechnology, 3(1), 015006.

34. Karayunlu S., Ay U., Spectrophotometric Determination of Total Inorganic Arsenic with Hexamethylene Ammonium Hexamethylenedithiocarbamate in Non-ionic Triton X100 Micellar Media, ISSN 10619348, Journal of Analytical Chemistry, 2010, Vol. 65, No. 3, pp. 244–248.

35. McCarthy J. R., Weissleder R., Multifunctional magnetic nanoparticles for targeted imaging and therapy, Adv. Drug Delivery Rev. 60(11)(2008) 1241–1251.

36. McCarthy J. R., Kelly K. A., Sun E. Y., Weissleder R., Targeted delivery of multifunctional magnetic nanoparticles, Nanomedicine2 (2)(2007) 153–167.

37. Kaushik A., Khan R., Solanki P. R., Pandey P., Alam J., Ahmad S., Malhotra B.D., Iron oxide nanoparticles-chitosan composite based gluscose biosensor, Elseiver, Volume 24, Issue 4, 1 December 2008, 676–683.

38. Castelloo J., Gallardo M., Busquets M. A., Estelrich J., Chitosan (or alginate)-coated iron oxide nanoparticles: A comparative study, Elseiver, Volume 468, 5 March 2015, 151–158.

39. Joshi A., Chaudhuri M., Removal of Arsenic from groundwater by iron oxide coated sand, J. Environ. Eng., 122(8), 769–771.

40. Shipley H. J., Engates K. E., Guettner A. M., Study of iron oxide nanoparticles in soil for remediation of arsenic, J Nanopart Res (2011) 13:2387–2397